Frontiers of Physics
https://doi.org/10.1007/s11467-019-0883-6
Front. Phys.
14(4), 43501 (2019)

LETTER

Large magnetocaloric effect in van der Waals crystal $CrBr_3$

Xiaoyun Yu[1], Xiao Zhang[1,†], Qi Shi[1], Shangjie Tian[2], Hechang Lei[2,‡], Kun Xu[1], Hideo Hosono[3,4]

[1] *State Key Laboratory of Information Photonics and Optical Communications & School of Science, Beijing University of Posts and Telecommunications, Beijing 100876, China*
[2] *Department of Physics and Beijing Key Laboratory of Opto-electronic Functional Materials & Micro-nano Devices, Renmin University of China, Beijing 100872, China*
[3] *Materials Research Center for Element Strategy, Tokyo Institute of Technology (MCES), Yokohama, Kanagawa 226-8503, Japan*
[4] *Materials and Structures Laboratory, Tokyo Institute of Technology, Yokohama, Kanagawa 226-8503, Japan*
Corresponding authors. E-mail: †*zhangxiaobupt@bupt.edu.cn,* ‡*hlei@ruc.edu.cn*
Received November 18, 2018; accepted January 4, 2019

We study the magnetocaloric effect (MCE) in van der Waals (vdW) crystal $CrBr_3$. Bulk $CrBr_3$ exhibits a second-order paramagnetic-ferromagnetic phase transition with $T_C = 33$ K. The maximum magnetic entropy change $-\Delta S_M$ near T_C is about 7.2 J·kg^{-1}·K^{-1} with the maximum adiabatic temperature change $\Delta T_{\rm ad}^{\rm max} = 2.37$ K and the relative cooling power RCP = 191.5 J·kg^{-1} at $\mu_0 H = 5$ T, all of which are remarkably larger than those in CrI_3. These results suggest that the vdW crystal $CrBr_3$ is a promising candidate for the low-dimensional magnetic refrigeration in low temperature region.

Keywords magnetocaloric effect, 2D magnetic materials

The discovery of two-dimensional (2D) van der Waals (vdW) materials has stimulated extensive research interest for basic science and applied technologies [1]. Owing to the reduced dimensionality, 2D materials with atomic thickness manifest unique physical properties, distinct from conventional bulk materials. For example, bulk MoS_2 is an indirect band gap semiconductor but it becomes a direct band gap one when thinning down to monolayer [2]. These features are utterly important for novel optoelectronic devices [1]. Among the various novel properties of 2D vdW materials, 2D ferromagnetism is a long-sought one. The absence of 2D vdW crystals with intrinsic magnetism has hindered the development of new magnetic, magnetoelectric and magneto-optic applications. Very recently, the long-range ferromagnetism with Curie temperature T_C of 45 K in the monolayer CrI_3 has been observed [3]. It indicates that the ferromagnetism in bulk materials can be retained even in monolayer ones. This discovery sheds light on exploring novel 2D ferromagnetic (FM) materials [3].

Layered chromium halides CrX_3 (X = Cl, Br, and I) have the same rhombohedral BiI_3-type structure (space group $R\bar{3}$, No. 148) at low temperatures [4, 5]. Taking $CrBr_3$ as an example [Fig. 1(a)], the edge-shared CrBr6 octahedra form a 2D honeycomb layers of Cr ions and these [CrBr] slabs are stacked along the c axis with vdW gaps in between. The cleavage energies of these three compounds are comparable to graphite and MoS_2 [4, 5]. Each of CrX_3 compounds is a magnetic semiconductor with a small band gap. But the different radii of halides alter the in-plane nearest-neighbor Cr-Cr distance and the vdW gap between [CrX] slabs, leading to the changes of magnetic interactions in these materials. As a result, $CrCl_3$ displays antiferromagnetic with Neel temperature T_N of 16.8 K, while $CrBr_3$ and CrI_3 show ferromagnetism with $T_C = 33$ K and 68 K [4–6]. All of these materials are magnetic semiconductors.

Among various properties of FM materials, magnetocaloric effect (MCE) is an important one that can be used for magnetic refrigeration, a promising, environmentally friendly energy-conversion technology. Even the MCE of many materials have been studied for a long time, the MCE in the FM vdW materials are still rare. $Fe_{3-x}GeTe_2$ with $T_C = 225$ K shows the maximum values of magnetic entropy change $-\Delta S_M^{\rm max}$ is about 1.1 J·kg^{-1}·K^{-1} at 5 T [7]. CrI_3 exhibits anisotropic $-\Delta S_M^{\rm max}$ with the values of 4.24 and 2.68 J·kg^{-1}·K^{-1} at 5 T for $H//c$ and $H//ab$, respectively [8]. In this work, we carried out a study on the MCE of $CrBr_3$ single crystal. The $CrBr_3$ undergoes a second-order phase transition in the vicinity of T_C and the $-\Delta S_M^{\rm max}$ is about 7.2 J·kg^{-1}·K^{-1} at 5 T, much larger than that of the homologous series CrI_3. Due to such large MCE, this compound would be a promising candidate material for magnetic refrigeration at low temperature.

Single crystals of $CrBr_3$ were grown by chemical vapor transport method with the mixture of polycrystal $CrBr_3$ (99 %) powder. The starting materials were sealed in a silica tube under vacuum and then placed inside a two-zone horizontal tube furnace with temperature up to 890

K and 773 K for 7 days. The shiny black plate-like crystals with lateral dimensions up to several millimeters can be obtained. The X-ray diffraction (XRD) data were taken using a Bruker D8 X-ray diffractometer with Cu K_α radiation ($\lambda = 0.15418$ nm) at room temperature. The elemental analysis was performed using the energy-dispersive X-ray spectroscopy (EDX). Heat capacity was measured using a Quantum Design physical property measurement system (PPMS9). Magnetic properties were measured using a Quantum Design magnetic property measurement system (MPMS3). During the measurements, a piece of $CrBr_3$ single crystal was mounted in a plastic straw for both field directions. The crystal is about 0.6 mg with the sample geometry of 0.3 mm × 0.24 mm × 0.2 mm ($a \times b \times c$). For the M(H) measurement when $H//c$, the magnetic field has been corrected by using the formula $\mu_0 H = \mu_0 H - 4\pi N M$, where N is the demagnetization factor (~ 0.84). For the M(H) measurement when $H//ab$, the N is negligible (~ 0.07), thus the external magnetic field is not corrected.

As shown in Fig. 1(b), $CrBr_3$ single crystal has a plate-like morphology, consistent with its layered structure. The reflections in the XRD pattern of a single crystal [Fig. 1(c)] can be well indexed by the indices of $(00l)$ lattice plane, indicating that the surface of crystal is perpendicular to the c axis (parallel to the ab plane). The EDX spectrum of a $CrBr_3$ single crystal confirms the existence of Cr and Br and the determined average atomic ratio of Cr to Br is 1:3.38(4), close to the chemical formula of $CrBr_3$. Moreover, the absence of other elements in the EDX spectrum also indicates the high purity of $CrBr_3$ crystals.

Figure 2(a) shows the temperature dependence of magnetization $M(T)$ at $\mu_0 H = 0.1$ T for $H//c$ and $H//ab$ with zero-field-cooling (ZFC) and field-cooling (FC) modes. For both field directions, the $M(T)$ curves exhibit rapid increase at low temperature, corresponding to the paramagnetic to FM phase transition and the T_C determined from the peak of derivative $d\chi(T)/dT$ is about 33 K, close to that reported in the literature [6]. Moreover, it can be seen that when $T < T_C$, the $M(T)$ for $H//ab$ drops gradually with decreasing temperature in contrast to the $M(T)$ for $H//c$ which is almost insensitive to temperature. Similar behavior has also been observed in CrI_3 [5], suggesting that the easy axis of magnetization is along the c axis. In addition, the ZFC and FC $M(T)$ curves for both field directions are overlapped very well in the whole measuring temperature range, implying the absence of spin glassy behavior in $CrBr_3$. On the other hand, the magnetic susceptibility $\chi(T)$ curve for $H//c$ measured with FC mode was fitted by the modified Curie–Weiss law $\chi = \chi_0 + C/(T - \theta)$ in the temperature range between 150 and 300 K (inset of Fig. 2(a)), where χ_0 is a temperature-independent term, C is the Curie constant and θ is the Weiss temperature. The estimated value of θ is 49.7(1) K, confirming the FM interaction between Cr ions. Moreover, the obtained value of C is 0.1917(4) emu·K·mol^{-1}·T^{-1}, corresponding to the effective magnetic moment $\mu_{\text{eff}} = 3.906(4)\ \mu_B$/Cr. It is very close to the expected value $\mu_{\text{eff}} = 3.87\mu_B$ for spin-only Cr^{3+} ion ($S = 3/2$). Figure 2(b) shows the isothermal $M(H)$ curves measured at 2 K for both field directions. The values of saturation field is about 0.36 and 0.8 T for $H//c$ and $H//ab$, respectively. The smaller value of the former indicates that the easy axis is the c axis, in agreement with the results of $M(T)$ curves. But a small difference between two values implies that $CrBr_3$ does not have a strong uniaxial anisotropy, unlike that in CrI_3 [5].

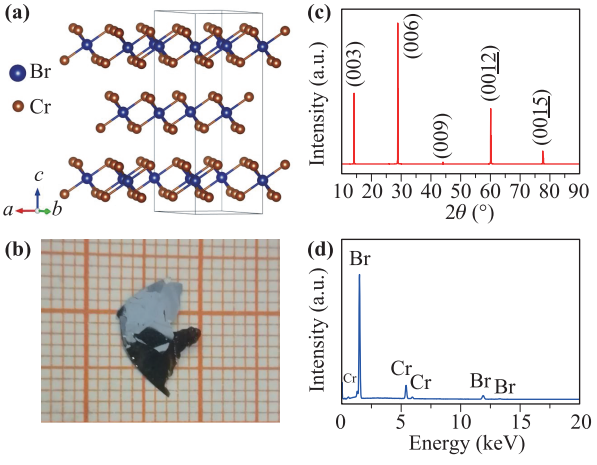

Fig. 1 **(a)** Crystal structure of $CrBr_3$ with Cr, Br represented by the brown and blue balls, respectively. **(b)** Photo of thin and flexible platelet $CrBr_3$ single crystal. The length of one grid in the photo is 1 mm. **(c)** XRD pattern and **(d)** EDX result of a $CrBr_3$ single crystal.

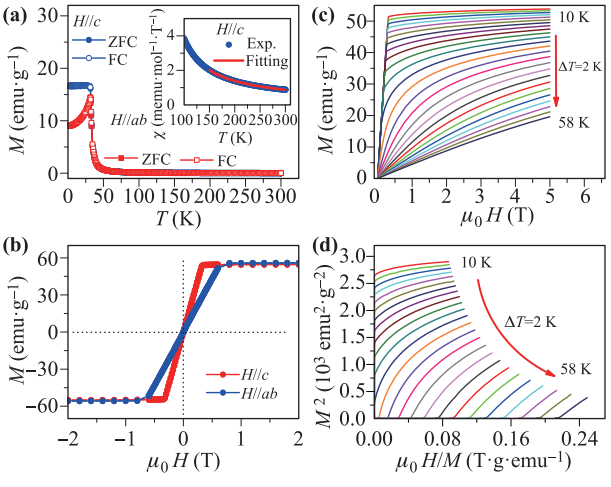

Fig. 2 **(a)** Temperature dependence of $M(T)$ at $\mu_0 H = 0.1$ T for $H//c$ and $H//ab$ with ZFC and FC modes. Inset: Temperature dependence of $\chi(T)$ at $\mu_0 H = 0.1$ T. The solid line represents the fit using the modified Curie-Weiss law in the temperature range between 150 and 300 K. **(b)** The isothermal $M(H)$ curves measured at 2 K for $H//c$ and $H//ab$. **(c)** The initial isothermal $M(H)$ curves around T_C for $H//c$. **(d)** Arrott plot with mean field model.

Moreover, the quiet small remanet magnetizations and coercivity fields for both field directions suggest the soft ferromagnetism of $CrBr_3$, consistent with the weak magnetic anisotropy in this material. Importantly, this soft magnetism will lead to minimal hysteresis losses that would be detrimental to the cooling effect. On the other hand, the saturation moment at 2 K is about 2.85 μ_B/Cr, close to the theoretical value $gS = 3\mu_B$ for Cr^{3+} ion with considering spin contribution only.

Figure 2(c) exhibits the initial isothermal magnetization curves $M(H)$ in the magnetic field up to 5 T from 10 K to 58 K with a temperature step of 2 K. When $T > T_C$, the curves are almost linear, indicating a PM behavior. With decreasing temperature, the curves become bending with negative curvatures, suggesting an FM interaction appears. When T is far below T_C, there is a sharp increase in the $M(H)$ curve in low-field region and then the magnetic moment saturates in high-field region, a typical feature of ferromagnet. In order to illustrate the order of PM–FM transition in $CrBr_3$, the relationship between M^2 and H/M, known as the Arrott plot, is shown in Fig. 2(d). Apparently, the slopes for all of curves in high-field region is positive, clearly indicating that the PM–FM phase transition is second-order [9, 10]. Moreover, these curves at various T are not parallel to each other with constant slope in the high-field region. It implies that the mean-field theory can not describe the critical behavior of $CrBr_3$ near T_C.

According to the classical thermodynamical and the Maxwell's thermodynamic relation, the isothermal magnetic entropy change $-\Delta S_M(T)$ associated with the external field is given by [11, 12]

$$\Delta S_M(T,H) = \int_0^H \left(\frac{\partial S}{\partial H}\right)_T \mathrm{d}H = \int_0^H \left(\frac{\partial M}{\partial T}\right)_H \mathrm{d}H, \tag{1}$$

where $(\frac{\partial S}{\partial H})_T = (\frac{\partial M}{\partial T})_H$ is based on Maxwell's relation. Under discrete magnetization and temperature measurements, $-\Delta S_M$ can be approximated written as

$$|\Delta S_M(T,H)| = -\sum \left[\frac{(M_{i+1} - M_i)}{T_{i+1} - T_i}\right] \Delta H_i, \tag{2}$$

where M_i and M_{i+1} are the magnetization at T_i and T_{i+1} under the same magnetic field, respectively [11, 12]. The evolution of isothermal magnetic entropy changes $-\Delta S_M$ as functions of magnetic field and temperature is presented in Fig. 3(a). The curve of $-\Delta S_M$ at certain field shows a peak in the vicinity of T_C and the absolute value of $-\Delta S_M$ becomes larger with increasing field. The maximum value of magnetic entropy changes $-\Delta S_M^{\max}$ at $\mu_0 H = 5$ T is about 7.2 J·kg^{-1}·K^{-1} (33.0 mJ·cm^{-3}·K^{-1}). Recent studies proposed that for a second-order PM–FM transition, there is a scaling behavior between normalized magnetic entropy change $-\Delta S_M / -\Delta S_M^{\max}$ and rescaled temperature [13, 14]. The temperature axis was rescaled in a different way below and above T_C with an imposed constraint

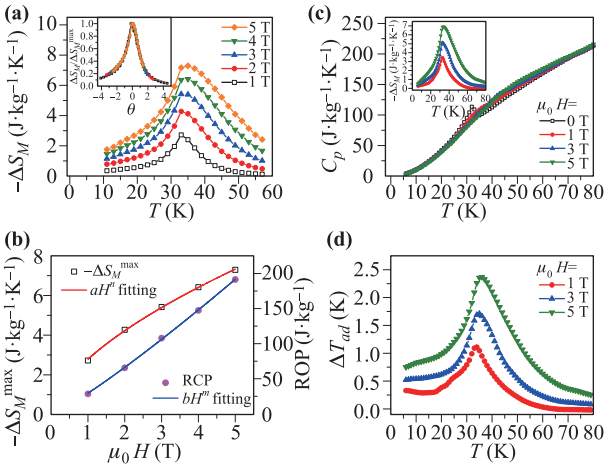

Fig. 3 **(a)** Magnetic entropy changes $-\Delta S_M$ at various fields. Inset: Universal behavior of the scaled entropy change curves at magnetic fields ranging from 1 to 5 T. **(b)** The $-\Delta S_M^{\max}$ and RCP as a function of H. The sold lines represent the power-law fittings. **(c)** Temperature dependence of heat capacity $C_p(T)$ at various fields. Inset: $-\Delta S_M$ obtained from heat capacity measurements. **(d)** Adiabatic temperature change ΔT_{ad} of $CrBr_3$.

that the position of the two reference points of each curve corresponds to $\theta = \pm 1$,

$$\theta = \begin{cases} -(T - T_C)/(T_{r1} - T_C), & \text{for } T \le T_C, \\ (T - T_C)/(T_{r2} - T_C), & \text{for } T > T_C, \end{cases} \tag{3}$$

where the reference temperatures T_{r1} and T_{r2} are chosen in order to make $-\Delta S_M(T_{r1}, T_{r2}) = -1/2\Delta S_M^{\max}$. It can be clearly seen that the curves of $-\Delta S_M(T,H)$ at different fields fall onto a single curve [inset of Fig. 3(a)], i.e., exhibiting a scaling behavior. It confirms the feature of second-order PM–FM transition in $CrBr_3$.

Another parameter to characterize the potential magnetocaloric effect of materials is the relative cooling power (RCP). It can be calculated using the expression [12]

$$\mathrm{RCP} = |\Delta S_M^{\max}| \times \delta T_{\mathrm{FWHM}}, \tag{4}$$

where the FWHM means the full width at half maximum of $-\Delta S_M$ curve. The δT_{FWHM} representing the temperature range of magnetic entropy change play an important role in the refrigeration capacity. The value of RCP reaches a maximum value of 191.5 J·kg^{-1} (0.877 J·cm^{-3}) at $\mu_0 H = 5$ T [Fig. 3(b)]. In addition, the field dependence of $-\Delta S_M^{\max}$ and RCP can be fitted very well by using the power-law relations $-\Delta S_M^{\max} \propto aH^n$ and RCP $\propto bH^m$ [Fig. 3(b)]. The fitted n and m is 0.60(1) and 1.15(2), respectively, deviating from the mean-field values 2/3 and 1.33, but close to the values for 3D XY or 3D Ising models [8, 13–15].

Figure 3(c) exhibits temperature dependence of heat capacity C_p at different fields. At zero field, there is a sharp jump at about 32 K, clearly indicating a bulk PM–FM

transition in $CrBr_3$. It is consistent with the $M(T)$ results. With increasing field, the jump starts to broaden and shifts to higher temperatures. This is a typical behavior of PM–FM transition. The entropy $S(T,H)$ can be calculated from the heat capacity as

$$S(T,H) = \int_0^T \frac{C_p(T,H)}{T} \mathrm{d}T + S_0(H), \quad (5)$$

where $S_0(H)$ is the zero-temperature entropy, which can be neglected in a condensed system [11]. If assuming the heat capacities of electronic and lattice are not sensitive to field, the $-\Delta S_M$ can be obtained using the formula $-\Delta S_M = S_M(T,H) - S_M(T,0)$. As shown in the inset of Fig. 3(c), the $-\Delta S_M(T)$ show similar temperature dependence to those derived from $M(H)$ curves and the $-\Delta S_M^{\max}$ at 5 T (~ 6.91 J·kg^{-1}·K^{-1}) is also in agreement with that value obtained from magnetization data. The adiabatic temperature change $\Delta T_{\mathrm{ad}}(= T(S,H) - T(S,0))$ caused by the field change during the isentropic process can be estimated from the heat capacity measurements. The temperature dependence of ΔT_{ad} shows a peak close to the T_C, similar to the $-\Delta S_M$ curves [Fig. 3(d)]. The $\Delta T_{\mathrm{ad}}^{\max}$ increases with increasing field and the $\Delta T_{\mathrm{ad}}^{\max}$ at 5 T is about 2.37 K.

The $-\Delta S_M^{\max}$ of $CrBr_3$ is significantly smaller than that of well-known magnetic refrigerating materials with first-order magnetic phase transition, such as $Gd_5Si_2Ge_2$, $LaF_{13-x}Si_x$, and $MnP_{1-x}As_x$ [16]. However, the first-order magnetic phase transition always accompanies by the lattice expansion and magnetic thermal hysteresis, that may reduce the physically achievable efficiency and hinders practical application. In contrast, the MCE parameters of $CrBr_3$ are comparable or even larger than those magnetic refrigerating materials with second-order phase transition. For example, the $-\Delta S_M^{\max}$ of $RE_6Co_{1.67}Si_3$ (RE = Pr, Gd, and Tb) are 6.9, 5.2 and 7.0 J·kg^{-1}·K^{-1} at 5 T, and for the sulfospinels $CdCr_2S_4$, this value is 7.0 J·kg^{-1}·K^{-1} at the same field [17]. Importantly, when compared to these materials, $CrBr_3$, as a binary compound, does not include costly rare-earth elements and is also easy to synthesis. It is worth noting that the values of $-\Delta S_M^{\max}$, RCP and $\Delta T_{\mathrm{ad}}^{\max}$ of $CrBr_3$ are also much larger than those values in CrI_3 at same field (~ 4.24 J·kg^{-1}·K^{-1}, 122.6 J·kg^{-1}, and 1.5 K at 5 T) [8]. Even using the unit of mJ·cm^{-3}·K^{-1} which is meaningful for practical application, the $-\Delta S_M^{\max}$ of $CrBr_3$ (33.0 mJ·cm^{-3}·K^{-1}) is still larger than that of CrI_3 (22.6 mJ·cm^{-3}·K^{-1}). This result shows that the variation of anions may have a significant influence not only on the T_C but also on the MCE. Thus, $CrBr_3$ could be a promising candidate for cryogenic magnetic refrigerating materials. Moreover, combining with the unique features of layered CrX_3, such as easy exfoliation down to a few layers or monolayer, persistence of 2D FM, maneuverable magnetism by using the external electric field [18–20], these kinds of vdW materials pave a way to study on the low-dimensional MCE and the interplay between MCE and other physical properties in 2D materials, especially in 2D heterostructures.

In summary, the magnetism and MCE of bulk $CrBr_3$ single crystal are comprehensively studied in the vicinity of the PM–FM transition. The PM–FM transition is second-order, confirmed by the analysis of Arrot plot and scaling behavior of $-\Delta S_M$. The $CrBr_3$ displays larger magnetic entropy changes near T_C and the $-\Delta S_M$ reaches the maximum values of 7.2 J·kg^{-1}·K^{-1} for $\Delta H = 5$ T, much larger than that in CrI_3. Combining with the easy exfoliation down to monolayer and large MCE, CrX_3 provides a new ingredient for the study of 2D materials.

Acknowledgements This work was supported by the Ministry of Science and Technology of China (No. 2016YFA0300504); the National Natural Science Foundation of China (Nos. 11574394, 11774423, and 11822412); the Research Funds of Renmin University of China (RUC) (Nos. 15XNLF06, 15XNLQ07, and 18XNLG14); the Fundamental Research Funds for the Central Universities (No. 2017RC20); the Research Innovation Fund for College Students of Beijing University of Posts and Telecommunications; and the Collaborative Research Project of Laboratory for Materials and Structures, Institute of Innovative Research, Tokyo Institute of Technology. H. H. was supported by the MEXT Elements Strategy Initiative to Form Core Research Center.

References

1. K. S. Novoselov, A. Mishchenko, A. Carvalho, and A. H. Castro Neto, 2D materials and van der Waals heterostructures, *Science* 353(6298), 461 (2016)
2. K. F. Mak, C. Lee, J. Hone, J. Shan, and T. F. Heinz, Atomically thin MoS_2: A new direct-gap semiconductor, *Phys. Rev. Lett.* 105(13), 136805 (2010)
3. B. Huang, G. Clark, E. Navarro-Moratalla, D. R. Klein, R. Cheng, K. L. Seyler, D. Zhong, E. Schmidgall, M. A. McGuire, D. H. Cobden, W. Yao, D. Xiao, P. Jarillo-Herrero, and X. Xu, Layer-dependent ferromagnetism in a van der Waals crystal down to the monolayer limit, *Nature* 546(7657), 270 (2017)
4. M. A. McGuire, G. Clark, S. Kc, W. M. Chance, G. E. Jellison, V. R. Cooper, X. Xu, and B. C. Sales, Magnetic behavior and spin-lattice coupling in cleavable van der Waals layered $CrCl_3$ crystals, *Phys. Rev. Mater.* 1(1), 014001 (2017)
5. M. A. McGuire, H. Dixit, V. R. Cooper, and B. C. Sales, Coupling of crystal structure and magnetism in the layered, ferromagnetic insulator CrI_3, *Chem. Mater.* 27(2), 612 (2015)
6. I. Tsubokawa, On the magnetic properties of a $CrBr_3$ single crystal, *J. Phys. Soc. Jpn.* 15(9), 1664 (1960)
7. V. Y. Verchenko, A. A. Tsirlin, A. V. Sobolev, I. A. Presniakov, and A. V. Shevelkov, Ferromagnetic order, strong magnetocrystalline anisotropy, and magnetocaloric effect in the layered telluride $Fe_{3-d}GeTe_2$, *Inorg. Chem.* 54(17), 8598 (2015)

8. Y. Liu and C. Petrovic, Anisotropic magnetocaloric effect in single crystals of CrI_3, *Phys. Rev. B* 97(17), 174418 (2018)
9. S. K. Banerjee, On a generalised approach to first and second order magnetic transitions, *Phys. Lett.* 12(1), 16 (1964)
10. X. Zhang, S. Matsuishi, and H. Hosono, Critical behavior and magnetocaloric effect in layered structure Tb_2C, *J. Phys. D* 49(33), 335002 (2016)
11. V. K. Pecharsky and K. A. Jr Gschneidner, Magnetocaloric effect from indirect measurements: Magnetization and heat capacity, *J. Appl. Phys.* 86(1), 565 (1999)
12. K. A. Jr Gschneidner and V. K. Pecharsky, Magnetocaloric materials, *Annu. Rev. Mater. Sci.* 30(1), 387 (2000)
13. V. Franco, J. S. Blázquez, and A. Conde, Field dependence of the magnetocaloric effect in materials with a second order phase transition: A master curve for the magnetic entropy change, *Appl. Phys. Lett.* 89(22), 222512 (2006)
14. V. Franco and A. Conde, Scaling laws for the magnetocaloric effect in second order phase transitions: From physics to applications for the characterization of materials, *Int. J. Refrig.* 33(3), 465 (2010)
15. H. Oesterreicher and F. T. Parker, Magnetic cooling near Curie temperatures above 300 K, *J. Appl. Phys.* 55(12), 4334 (1984)
16. K. A. Jr Gschneidner, V. K. Pecharsky, and A. O. Tsokol, Recent developments in magnetocaloric materials, *Rep. Prog. Phys.* 68(6), 1479 (2005)
17. B. G. Shen, J. R. Sun, F. X. Hu, H. W. Zhang, and Z. H. Cheng, Recent progress in exploring magnetocaloric materials, *Adv. Mater.* 21(45), 4545 (2009)
18. B. Huang, G. Clark, D. R. Klein, D. MacNeill, E. Navarro-Moratalla, K. L. Seyler, and N. Wilson, M. A. M-cGuire, D. H. Cobden, D. Xiao, W. Yao, P. Jarillo-Herrero, and X. Xu, Electrical control of 2D magnetism in bilayer CrI_3, *Nat. Nanotech.* 13, 544 (2018)
19. S. Jiang, L. Li, Z. Wang, K. F. Mak, and J. Shan, Controlling magnetism in 2D CrI_3 by electrostatic doping, *Nat. Nanotech.* 13(7), 549 (2018)
20. Y. Deng, Y. Yu, Y. Song, J. Zhang, N. Z. Wang, Y. Z. Wu, J. Zhu, J. Wang, X. H. Chen, and Y. Zhang, Gate-tunable room-temperature ferromagnetism in two-dimensional Fe_3GeTe_2, arXiv: 1803.02038 (2018)